Journal of Physics: Conference Series **2265** (2022) 022106 doi:10.1088/1742-6596/2265/2/022106

# Lifetime fatigue response due to wake steering on a pair of utility-scale wind turbines

**Scott Dana, Hristo Ivanov and Paula Doubrawa**

National Renewable Energy Laboratory, 15013 Denver West Parkway, Golden, CO 80401, USA

Scott.Dana@nrel.gov, Hristo.Ivanov@nrel.gov, Paula.Doubrawa@nrel.gov

**Abstract**. Quantifying the impacts on turbine loads during wind farm control is an important consideration in assessing power production benefits. Wake steering controls aim to improve total wind farm performance by coordinating the control actions of individual turbines, wherein an upstream turbine is intentionally yawed at an offset angle from the measured wind direction. Consequently, this redirects its wake for improved power production and potentially reduces fatigue loads of the downstream turbines. This paper studies the lifetime fatigue loads associated with wake steering by using utility-scale wind turbine experimental data to conduct an analysis on a pair of wind turbines. This study was part of a large field experiment in which a group of five GE 1.5-MW SLE CWE turbines were selected as targets for conducting wake steering research. A standard loads instrumentation package and data acquisition system were installed on two turbines within the cluster to measure turbine fundamental loads. The time-series databases were used to calculate loads statistics as well as short-term and lifetime damage equivalent loads. Fatigue calculations followed the guidance in Annex H of the International Electrotechnical Commission standard 61400-1, Edition 4. Lifetime fatigue calculation results are presented in this analysis; three methods of assessing lifetime fatigue were used to determine percent difference for blade root moments, main shaft moments, main shaft torque, and tower top torque. For all three fatigue treatments, some components' lifetime fatigue increases for the controlled turbine; however, the downwind turbine experienced a reduction in lifetime fatigue and combined effect for the turbine pair results in a reduction of fatigue when wake steering controls are applied.

## 1. Introduction

Quantifying the effects of wind farm control on turbine loads is an important step in assessing its benefits. Wind farm controls aim to improve overall wind farm performance by coordinating the control actions of individual turbines. Wake steering, or wake redirection, is an example of this technique wherein an upstream turbine is intentionally misaligned from the actual wind direction. Consequently, this redirects the turbine's wake so that downstream turbines can experience increased power production with possible load mitigation as a secondary effect.

In recent years, several studies, both theoretical and experimental, have been conducted to quantify the benefits from wake redirection. Much of the focus has been on power production, with limited focus on loads and fatigue life. Most studies conclude that utilizing wake steering results in increased overall power production for a wind farm while also providing a basis for load reduction for downstream turbines depending on wind farm layout [1], [2], [3], [4], [5], [6], [7], [8]. Most past research based these conclusions on short-term damage equivalent loads (DELs).

At this stage, more research is needed on quantifying the impact of load effects over a turbine's lifetime. One study [9] aimed to address this knowledge gap by investigating the lifetime fatigue loads in an existing offshore wind farm using simulations where wake steering was applied. In this paper, a similar approach is taken to study lifetime fatigue loads; however, measured data from a pair of utility-scale wind turbines are used in the analysis, providing factual estimates of lifetime fatigue.

## 2. Field experiment

This study was part of a larger field experiment in which a group of five GE 1.5-MW SLE CWE turbines (rotor diameter of 77 m, hub height of 80 m, rated wind speed of 14 m/s) within a wind farm were selected as targets for conducting wake steering research. This site was characterized by a predominant wind direction from the northwest with seasonal summer winds coming from the south and southeast. In this configuration, the wake interactions between turbines T2, T3, and T4 were studied while T1 and T5 were used as reference turbines (Figure 1). The scope of the overall field campaign was centered around applying wake steering controls to T2 and T4 and observing both individual effects to downstream turbines as well as overall performance across the pair of turbines affected by the controls.

As shown in Figure 1, several different types of instrumentation were deployed throughout the campaign. Measurements were collected from ground-profiling lidars, sodars, meteorological tower instrumentation, nacelle-mounted lidars, and wind turbine supervisory control and data acquisition (SCADA) systems. However, the focus of this paper involves analyzing the mechanical loads between T2 and T3 when wake steering controls are applied to T2 versus normal operation controls, with inflow coming from the northwest direction (figure 1). To accomplish this, both turbines were equipped with a loads instrumentation package. The quantities of interest that were measured and analyzed were tower top torque (strain gauges), yaw position (encoder), main shaft bending moments and torque (strain gauges), rotor azimuth (encoder), and blade root bending moments (strain gauges). Because there was no instrumentation that could measure the inflow downwind of T2, the nacelle-mounted cup anemometer and wind vane were used for T3. To be consistent, T2 also used its own nacelle-mounted cup and vane to measure inflow.

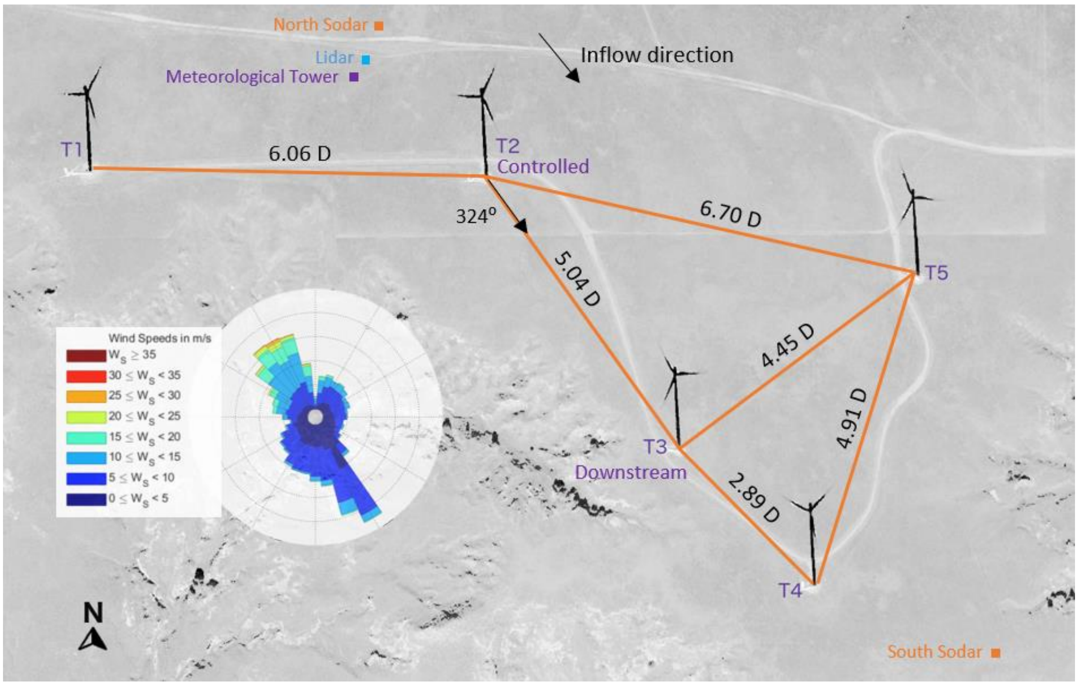


**Figure 1.** General site characteristics and instrumentation layout of a cluster of wind turbines in a wind farm [7].

## 3. Data collection and analysis methods

### *3.1. Data collection methods*

Raw data collected from instrumentation went through several stages of postprocessing and quality control. The data acquisition system (DAS) was based on a National Instruments PXI real-time scan engine paired with a custom-developed and validated LabVIEW code, which synchronously recorded all samples with GPS time stamps. All loads instrumentation, calibrations, and data collection were in accordance with International Electrotechnical Commission (IEC) standard 61400-13, Edition 1, 2015. A 50-Hz sample rate was used for recording and all data files were saved in 10-minute file lengths. For more detailed information on loads instrumentation and calibrations, see [10]. To facilitate the comparison between the upwind and downwind turbine pair, the recording times of T3 were time-synchronized with those of T2, resulting in identical starting time stamps of each recorded data file.

Data collection was governed by the application of wake steering controls to the upwind turbine (T2). The wind vane signal of T2 was modified to receive commands that resulted in a turbine yaw command response to a desired yaw offset. The commanded yaw offset followed a specific schedule based on wind speed and wind direction. The details of the schedule and controller logic can be found in [8]. The experiment was designed so that the modified wind vane controller of T2 alternated between on and off states of wake steering control on an hourly basis to arrive at data sets with comparable atmospheric conditions. Consequently, this resulted in two databases for each turbine where "baseline" refers to periods of conventional turbine controls without wake steering and "wake steering operation" (WSO) refers to periods when wake steering was enabled and the controller of T2 was sending yaw offset commands to T2 to facilitate desired yaw offsets for wake steering controls to improve power capture.

Throughout all the databases, several filters were applied to arrive at quality-controlled data, or valid data. All data files were filtered as follows:

- Only 50-Hz data rate files of 600 consecutive seconds were used.
- Removal of data when the T2 mean wind direction values were outside the range of 320°–350° true north (based on wake steering controller logic in [8]).
- Removal of data when the T2 DAS, T3 DAS, or wake steering controller was not functioning properly.
- Removal of data when the turbine SCADA status signals of T2 and T3 were not indicating a normal power production state (including derated operations).
- Removal of data when T2 or T3 active power was not greater than 0 kW.

Table 1 provides the wind speed bin totals of the resulting number of valid 10-minute time series collected for each database. Figure 2 provides a combined capture matrix, where turbulence intensity is quantified. Each square in the figure represents the number of 10-minute time series for each database permutation for the corresponding wind speed and turbulence intensity bin. The baseline databases for T2 and T3 had a total valid collection time of ~65 hours, while the WSO databases had a total time of ~68 hours.

**Table 1.** Wind speed bin totals of 10-minute time series data collected for each database.

| **Database** | **Wind Speed Bin [m/s]** | | | | | | | | | | | | | | | | | | |
|---|---|---|---|---|---|---|---|---|---|---|---|---|---|---|---|---|---|---|---|
| | ***0*** | ***3*** | ***4*** | ***5*** | ***6*** | ***7*** | ***8*** | ***9*** | ***10*** | ***11*** | ***12*** | ***13*** | ***14*** | ***15*** | ***16*** | ***17*** | ***18*** | ***19*** | ***20+*** |
| T2 Baseline | 1 | 5 | 5 | 14 | 19 | 14 | 18 | 6 | 14 | 38 | 86 | 59 | 40 | 26 | 26 | 11 | 6 | 1 | 0 |
| T2 WSO | 1 | 8 | 12 | 22 | 21 | 10 | 14 | 16 | 22 | 45 | 47 | 67 | 58 | 20 | 22 | 11 | 6 | 4 | 0 |
| T3 Baseline | 1 | 8 | 12 | 26 | 27 | 28 | 24 | 21 | 49 | 55 | 58 | 29 | 20 | 11 | 10 | 5 | 4 | 1 | 0 |
| T3 WSO | 0 | 10 | 22 | 25 | 28 | 17 | 19 | 34 | 33 | 68 | 70 | 33 | 20 | 8 | 7 | 4 | 7 | 1 | 0 |

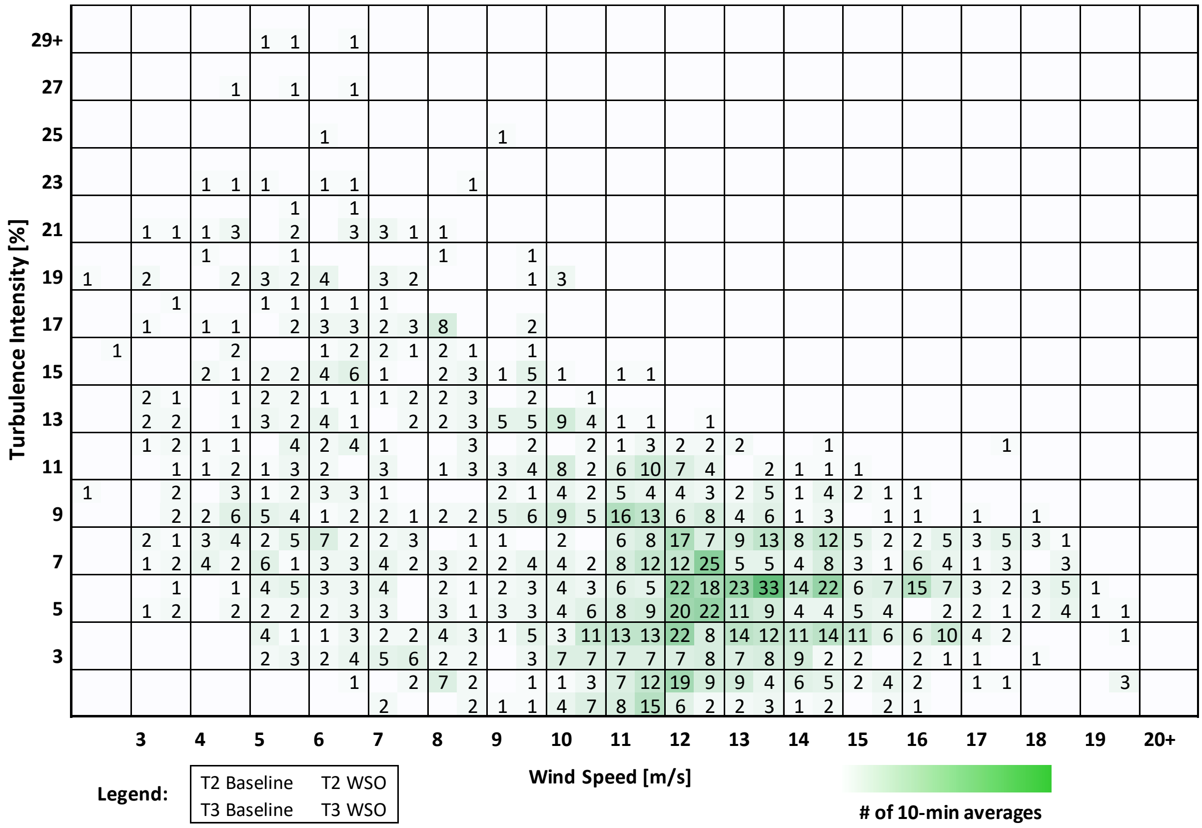


**Figure 2.** Combined capture matrix of 10-minute time series collected for each database.

### *3.2. Data analysis methods*

The procedures used to analyse the resulting databases are presented here. There were several steps taken to arrive at the results presented, including fatigue analysis, the method of load roses, and percent difference treatments of lifetime fatigue results.

*3.2.1. Fatigue analysis.* The time-series databases were used to calculate lifetime DELs. Fatigue calculations followed the guidance in Annex H of IEC 61400-1, Edition 4. The single-pass rainflow cycle counting method of Downing and Socie [11] was used with unclosed cycles counted as one-half (0.5). For lifetime fatigue calculations, a design life of 20 years and an equivalent frequency of 1 Hz was used with a Weibull mean wind speed of 8.5 m/s and shape factor of 2 (class II wind turbine). Material slopes used were 4 for steel components (tower and main shaft) and 10 for composite materials (blade root). The details of the lifetime fatigue theory used in this analysis can be found in [12].

*3.2.2. Load roses.* To better assess fatigue life of the load components, the technique of load roses was used. Load roses are used to divide a circular cross section into multiple sectors for improved spatial resolution of the loads acting on the wind turbine component. The local blade measurements were only able to sample the loading along two main directions, and it is unlikely that these coincide with the direction of maximum loading. Load roses allow estimation of the loading along other directions, thereby identifying the direction of greatest loading, which can then be used in further analyses. Figure 3 illustrates the load rose sections by angle and section number (e.g., "15°, LR 1", where 15° is the section located 15° from the 0° measurement location and LR stands for load rose) with the blade root and airfoil profiles for the maximum cord and the blade tip superimposed to better show the load rose sectors relative to the blade geometry. The airfoil profile shown is for example purposes only but illustrates the complexity of blade airfoil geometry and twist angles, which result in changes to the loading profile along the blade span where flap and edge measurements will not capture the complex loading of the circular blade root. The blade flap and edge moment orientations are indicated by $M_{bf}$ and $M_{be}$, respectively, relative to the load rose sectors.

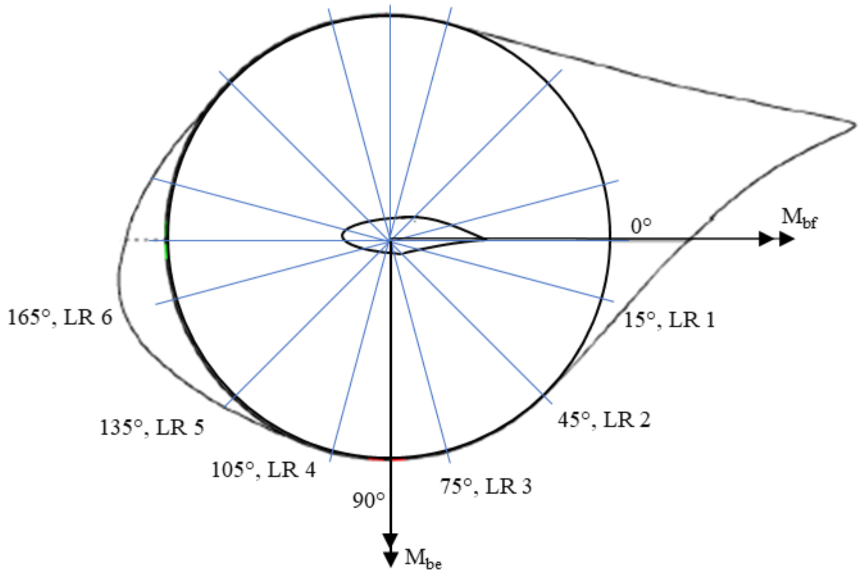


**Figure 3.** Load rose sectors and angle values used for fatigue analysis.

Only load rose sectors with the largest magnitude are used for further analysis and comparison with measured loads. To protect proprietary information, the lifetime DELs in Figure 4 are normalized by the maximum lifetime DEL across all blade load measurements ($M_{bf}$, $M_{be}$, and blade root resultant moment, Root $M_n$) and load roses, where LR 4 has the maximum value for Baseline operation, represented by unity (a value of one). All other blade DELs are normalized by this value. Blade root edge has a nearly identical fatigue life when compared to LR 4 for both WSO and baseline conditions. This is expected, as LR 4 is circumferentially close to the blade root edge moment direction (105° and 90°, respectively).

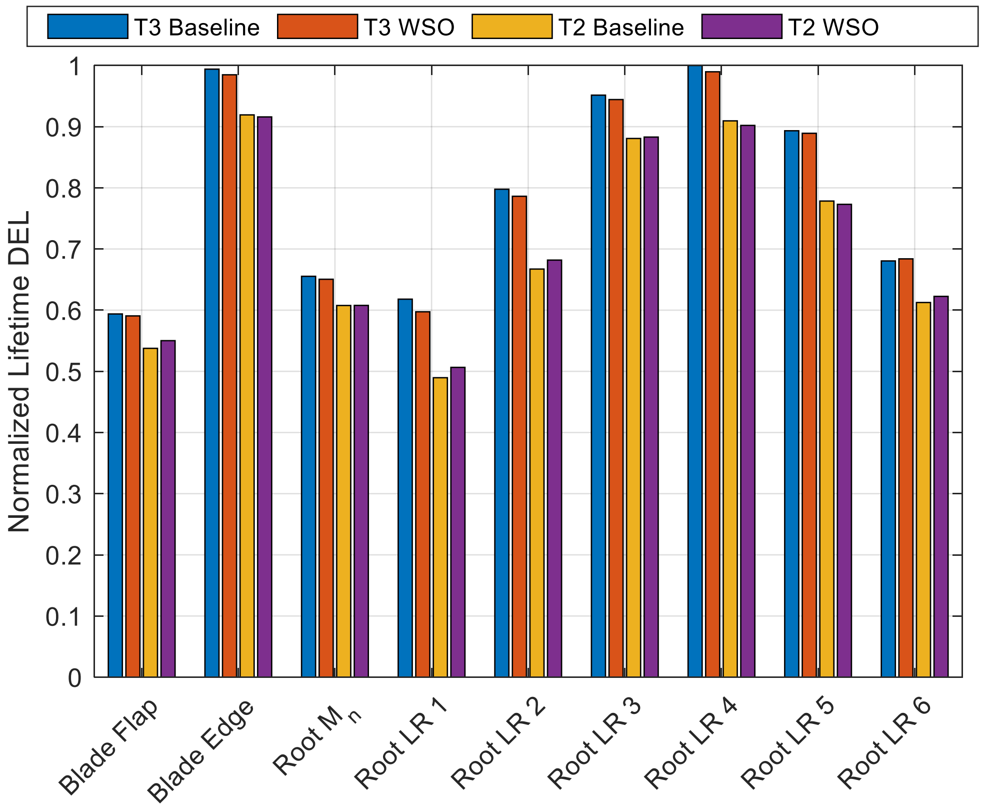


**Figure 4.** Blade root normalized lifetime DELs for identification of maximum fatigue direction.

The main shaft lifetime DELs were normalized with the maximum load component obtained at circular sector 3, determined using load to identify the largest lifetime fatigue value. This location (75° relative to main shaft 0°) is circumferentially near the main shaft pitch location (90°). Load roses were not used for the tower top torque, as torque is uniform over the circumferential cross section. Tower top torque serves as a proxy for yaw system fatigue and is essential to understanding the lifetime impact of wake steering controls to the design specifications of the yaw drive system (motors, gears, pucks, etc.).

*3.2.3. Lifetime fatigue comparison treatment.* To understand the lifetime fatigue impact of wake steering controls, three methods of assessing lifetime fatigue were used, as illustrated by the schematic in Figure 5.

Method 1 (M1) determined the percent difference between the wake steering controls (WSO) and the baseline controls for each turbine in reference to its own baseline lifetime fatigue. In this way, an increase in percent difference represents an increase in fatigue from normal operation, and vice versa. This allows the impact of wake steering controls to be assessed relative to each turbine's normal controls operation, irrespective of how the other turbine might be responding. Equation (1) shows the percent difference calculated for each turbine, where $DEL_{life,T2}$(WSO) and $DEL_{life,T2}$(Baseline) are the resulting lifetime DELs from the databases for T2 when wake steering controls are applied and for normal operation, respectively. Equation (2) is similar but is for T3.

$$M1_{\%Diff,T2} = [(DEL_{life,T2}(WSO) - DEL_{life,T2}(Baseline)) / DEL_{life,T2}(Baseline)] \times 100 \tag{1}$$

$$M1_{\%Diff,T3} = [(DEL_{life,T3}(WSO) - DEL_{life,T3}(Baseline)) / DEL_{life,T3}(Baseline)] \times 100 \tag{2}$$

Method 2 (M2) determined the percent difference of the summation of fatigue life for the pair of turbines for each wake steering condition (Baseline and WSO) referenced to the Baseline total lifetime fatigue. The rainflow cycles are concatenated between turbines to calculate lifetime fatigue for the pair of turbines in each wake steering control condition. This method results in a single set of percent difference values that quantifies the total change in lifetime fatigue to the pair of turbines due to wake steering controls. Equation (3) provides the percent difference calculation used, where $DEL_{life,Combined}$ is the combined lifetime fatigue result from the concatenated databases of T2 and T3 as a function of each operating case, WSO and Baseline:

$$M2_{\%Diff} = [(DEL_{life,Combined}(WSO) - DEL_{life,Combined}(Baseline)) / DEL_{life,Combined}(Baseline)] \times 100 \quad (3)$$

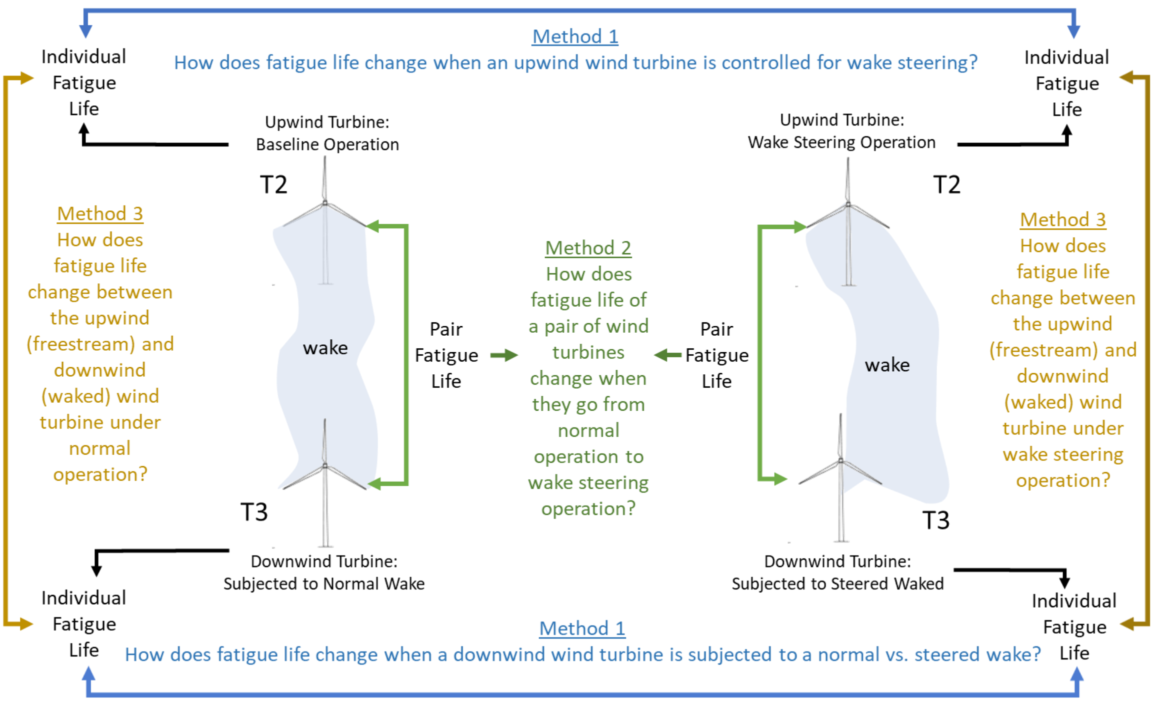


**Figure 5.** Schematic of the lifetime fatigue percent difference calculation methods.

Method 3 (M3) determined the percent difference between turbines for each wake steering condition referenced to T3. With this method the lifetime fatigue magnitudes between turbines are better represented. Whereas the first method captures the relative changes for each turbine due to wake steering controls, and the second method captures the total change of the pair due to wake steering, the third method determines the changes in fatigue between turbines (T2 and T3) and for each wake on/off condition (Baseline and WSO). An increase in percent difference is an increase in fatigue of T3; similarly, a decrease is a reduction in fatigue of T3. This process of evaluation quantifies the difference in lifetime fatigue between turbines and wake steering controls. Additionally, these results are scaled by the wake steering application factors to determine lifetime fatigue percent differences from baseline or normal operation (Section 4). Equation (4) demonstrates the percent difference calculation of Method 3 for the Baseline database when comparing between T2 and T3, where $DEL_{life,T3}(Baseline)$ is the lifetime DEL for T3 and $DEL_{life,T2}(Baseline)$ is the lifetime DEL for T2. Similarly, in equation (5), the percent difference calculation is shown for the WSO database, where $DEL_{life,T2}(WSO)$ is the wake steering operation lifetime DEL of T2, and, $DEL_{life,T3}(WSO)$ is the wake steering operation lifetime for T3.

$$M3_{\%Diff}(Baseline) = [DEL_{life,T3}(Baseline) - DEL_{life,T2}(Baseline)) / DEL_{life,T3}(Baseline)] \times 100 \quad (4)$$

$$M3_{\%Diff}(WSO) = [DEL_{life,T3}(WSO) - DEL_{life,T2}(WSO)) / DEL_{life,T3}(WSO)] \times 100 \quad (5)$$

## 4. Results

Lifetime fatigue percent difference results are presented for three different methods of comparison. The loads components presented include blade root flap (Blade Flap), blade root edge (Blade Edge), blade root resultant (Root $M_n$), blade root load rose maximum (Root LR Max), main shaft torque (MS Torque), main shaft pitch (MS Pitch), main shaft yaw (MS Yaw), main shaft resultant (MS $M_n$), main shaft load rose maximum (MS LR Max), and tower top torque (TT Torque). Blade root resultant is the resultant moment using the blade root edge and flap component loads. Similarly, main shaft resultant is the resultant moment of the main shaft using the pitch and yaw component loads.

Part of the results presented illustrate the influence of wake steering controls under the assumption of 100% annual operation with wake steering. This assumption would require T2 and T3 to maintain an annual wind direction alignment that was applicable to wake steering—the sector of 320°–350° true north for their specific arrangement (refer to the inset wind rose in figure 1). In practice, wake steering is applied based on wind direction, wind speed, and wind farm configuration. Given the historical wind speed and wind direction data for the wind turbines used in this study, wake steering is applicable approximately 16% of the year for this wind direction sector. This sector was calculated using 10-minute inflow averages in conjunction with the controller logic in [8]. To obtain a more realistic estimate of lifetime fatigue due to wake steering, the resulting percent difference values were scaled proportionately based on this value of 0.16 (a weighting of 16%) for the annual average WSO. Both a weighting of 1.00 (100% WSO) and 0.16 WSO percent difference results are presented against baseline operation 1.00 Baseline (0% WSO/100% Baseline) for comparison.

### *4.1. Method 1*

Figure 6 provides the results from Method 1 used to compare fatigue life. This method results in percent difference values due to wake steering for turbines T2 and T3. While T2 (the wake steering-controlled turbine) experiences an increase in lifetime fatigue compared to baseline operation, T3 (the downstream turbine) has nearly the opposite trend, demonstrating an improvement or reduction in lifetime fatigue. These trends are consistent with short-term fatigue results presented in [4] and [10]. The main shaft has the largest changes in lifetime fatigue for both WSO and Baseline operation.

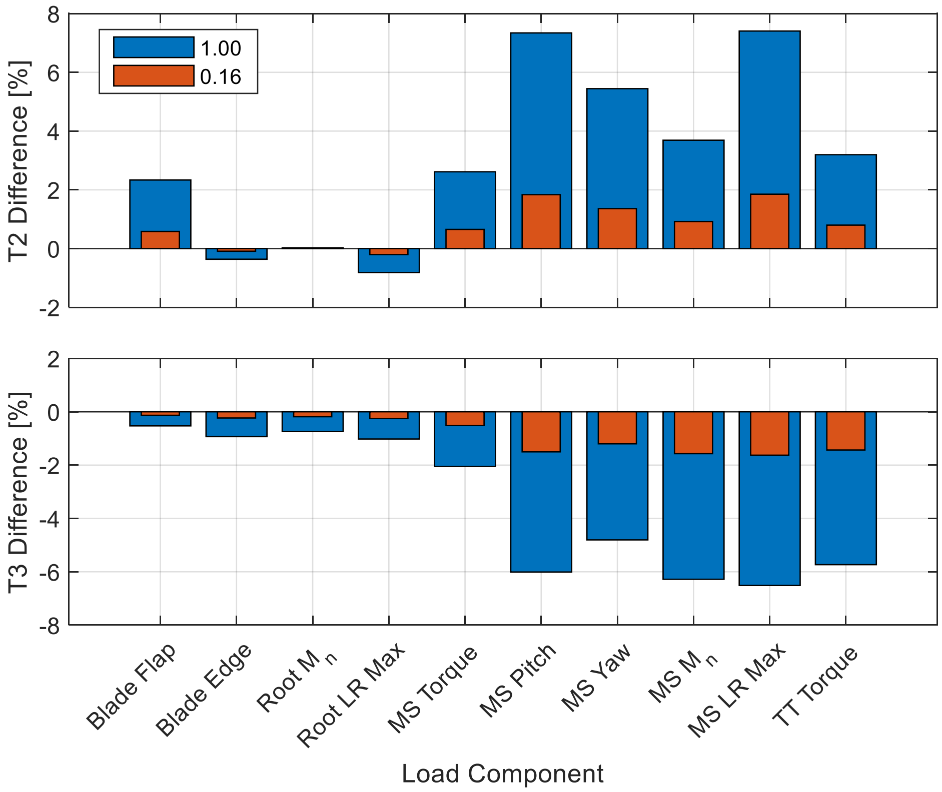


**Figure 6.** Turbine lifetime fatigue difference due to fraction of applied wake steering controls for each turbine.

### *4.2. Method 2*

The results of the second method used for lifetime fatigue comparison are shown in Figure 7. In this case, the lifetime fatigue is summed between turbines for the different wake steering control conditions. A percent difference is then derived in reference to baseline operation, yielding one set of values. For all components except blade flap, there is a small improvement in lifetime fatigue for the turbine pair. It should be noted that the edge moment drives fatigue loads and, in terms of magnitudes, is much larger than flap loads. Even with the modest increase in flap direction lifetime magnitude shown here, the total increase is much smaller in magnitude relative to the edge direction magnitude. Again, the main shaft has the largest change in fatigue life. When scaling the lifetime fatigue results by annual operation (0.16 weighting), the percent difference changes are less than 0.5% across all load signals considered, suggesting that wake steering controls have little influence on the total fatigue of the turbine pair. However, the global impact is seen as a small reduction in total fatigue.

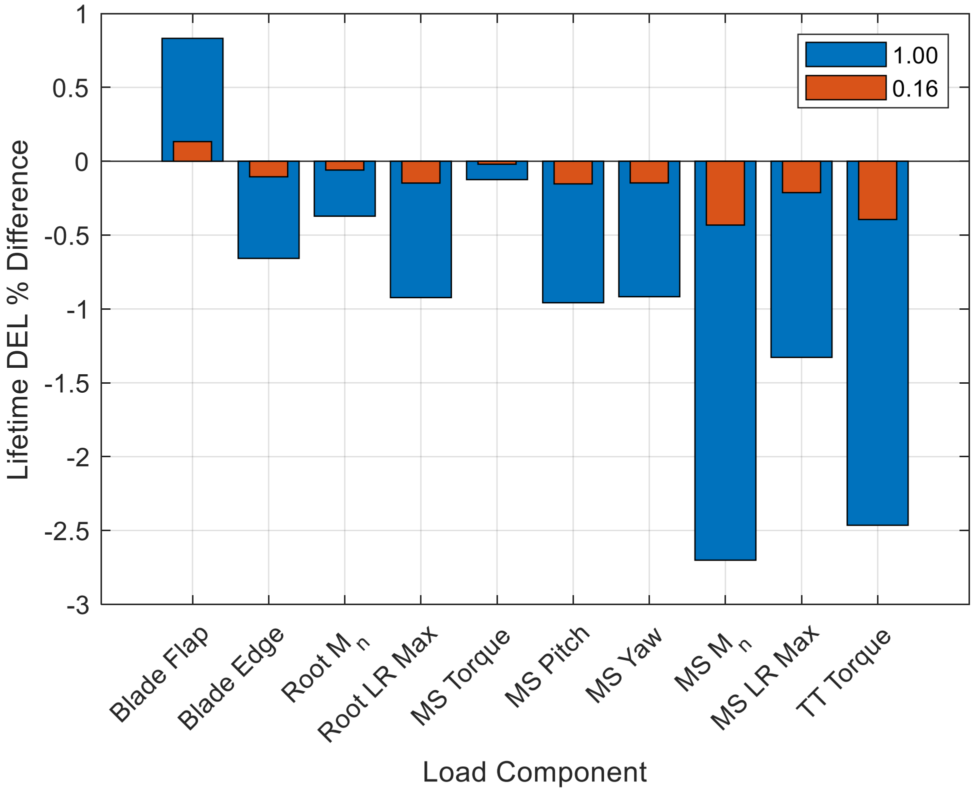


**Figure 7.** Lifetime fatigue difference for the turbine pair referenced to baseline operation (no wake steering controls).

### *4.3. Method 3*

The results from Method 3 are provided in Figure 8. Here, the magnitudes of the lifetime fatigue values are better represented, where T3 is always shown to experience larger lifetime fatigue results in comparison to T2, with the main shaft and tower top torque lifetime DELs nearly 40% larger by the percent difference calculation. However, the impact of wake steering controls to T2 (WSO) is still evident, as shown by the reduction in percent difference. The most notable improvements are seen on the main shaft components and tower top torque, on the order of 10%–15% for the 1.00 WSO weighting application. For 16% annual operation of WSO (0.16 weighting), the improvement to the percent difference result is smaller, as expected, but a benefit to lifetime fatigue is demonstrated.

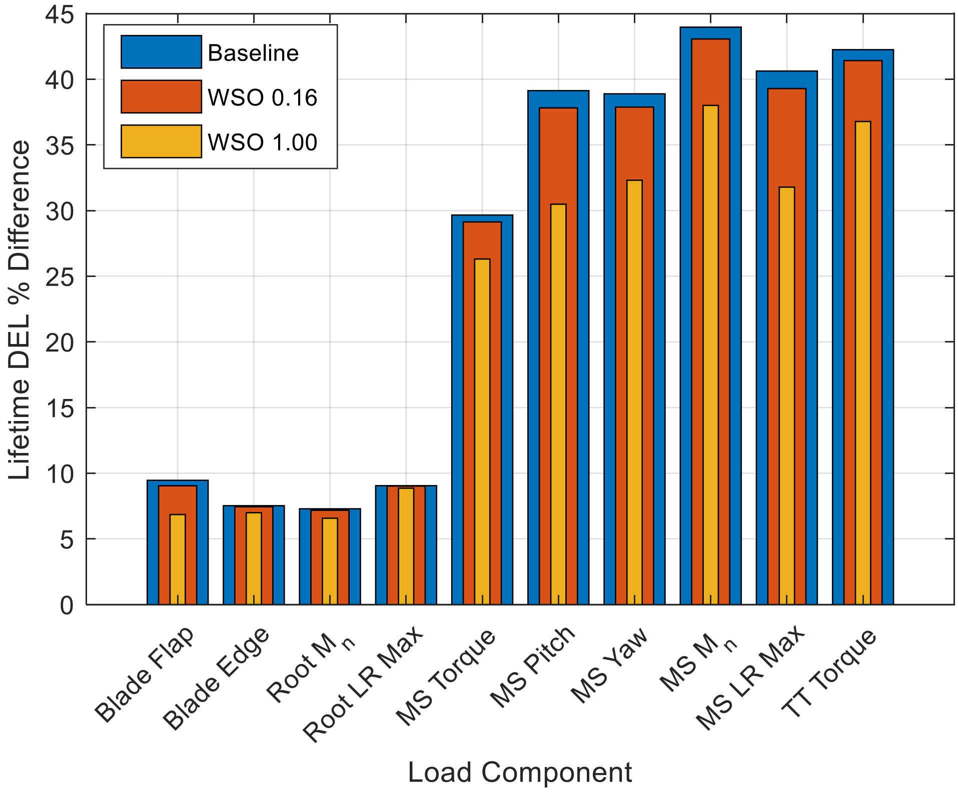


**Figure 8.** Turbine lifetime fatigue difference between turbines for each wake steering condition.

The results of Method 3 highlight the increased fatigue of the downwind turbine. The turbulence intensities and wind speeds presented in Figure 2 indicate that each turbine and operating state experienced very similar conditions, and the T3 fatigue results were likely not skewed by turbulence or high wind events. However, the turbulence was determined using a single-point measurement at the nacelle and lacks the spatial resolution to understand the wake propagation to the downwind turbine. The overall turbulence and inflow across the rotor disk of T3 is much different than the freestream inflow of T2. A better understanding of inflow, both in horizontal and vertical directions, is needed to fully assess rotor wake overlap effects and fatigue response. However, this result indicates the downwind turbine experiences greater fatigue compared to perimeter rows, even when the perimeter wind turbines are misaligned with respect to the incoming flow as in the case of wake steering.

## 5. Conclusions

Wake steering control is a technique used to improve wind farm performance by coordinating wake redirection where an upstream turbine's yaw orientation is commanded to an angle that is offset from the inflow wind direction. Limited studies have been conducted to demonstrate the loads response due to wake steering. To address this knowledge gap, a lifetime fatigue loads study was completed on a pair of utility-scale wind turbines using experimental data. Data were collected and carefully filtered for times of normal operation and wake steering controls.

Filtered data were processed to engineering units and analyzed for lifetime fatigue loads by the method of load roses and rainflow cycle counting. The resulting lifetime damage equivalent loads were further assessed using three percent-difference methods to quantify the impact of wake steering controls. Annual operation for the wind turbine pair was determined from historical data and used to weight the lifetime results for further determination of the effect of wake steering controls on lifetime fatigue.

The results clearly demonstrate that while some lifetime fatigue increases were shown for the wake steering-controlled turbine, the combined effect for the turbine pair from Method 3 reveals an overall reduction in lifetime fatigue. While the total lifetime fatigue shown in Method 3 can provide a measure of wake steering controls impact for the turbine pair, it is important to understand how each turbine's fatigue life changes due to wake steering controls. If a benefit to the downwind turbine results in an unacceptable detriment to the upwind turbine, the total change in lifetime fatigue can be misleading. Furthermore, the interior turbine loading environment is much different than the upwind controlled turbine and deserves more attention in future studies; however, a benefit from wake steering controls was demonstrated.

Altogether, the analysis revealed that percent difference changes to lifetime fatigue increase less than 8% for the largest load component, the main shaft, when wake steering controls are applicable for a 20-year design life (WSO 1.00). In practice, the annual usage of wake steering controls is much less for the wind farm configuration considered in this study, with an annual application of wake steering at 16% based on historical wind speed data for the turbine pair analyzed in this study and lifetime fatigue was scaled proportionately.

In summary, wake steering controls did not result in an adverse impact on turbine lifetime fatigue for the individual turbine or pair of turbines analyzed, and a net benefit in terms of lifetime fatigue for the pair of turbines in this study was shown to be possible.

**References**

[1] Gebraad P M O, Teeuwisse F W, van Wingerden W, Fleming P A, Ruben S D, Marden J R and Pao L Y 2016 *Wind Energy* **19** 95–114
[2] van Dijk T *et al.* 2016 *J. Phys.: Conf. Ser.* **753** 062013
[3] Campagnolo F, Petrovic V, Bottasso C and Croce A 2016 *American Control Conf.* 6–8 July 2016 Boston, MA, USA
[4] Damiani R, Dana S, Annoni J, Fleming P, Roadman J, van Dam J and Dykes K 2018 *Wind Energy Science* **3** 173–89
[5] White J, Ennis B, Herges T 2018 *Estimation of Rotor Loads Due to Wake Steering* American Institute of Aeronautics and Astronautics
[6] Brandon L Ennis *et al.* 2018 *J. Phys.: Conf. Ser.* **1037** 052001
[7] Fleming P *et al*. 2019 *Wind Energy Science* **4** 273–85
[8] Fleming P *et al*. 2020 *Wind Energy Science* **5** 945–58
[9] Kanev S, Bot E and Giles J 2020 *Energies* **13** 4088
[10] Ivanov H, Dana S and Doubrawa P 2021 *Loads response that is due to wake steering on a pair of utility-scale wind turbines* Golden, CO National Renewable Energy Laboratory Report
[11] Downing S and Socie D 1982 *Int. J. Fatigue* **4** 31–40
[12] Hayman G J 2012 *MLife theory manual for version 1.00* Golden, CO National Renewable Energy Laboratory Report